



# Global Analysis of Baculovirus Autographa californica Multiple Nucleopolyhedrovirus Gene Expression in the Midgut of the Lepidopteran Host *Trichoplusia ni*

Anita Shrestha,a Kan Bao,a Yun-Ru Chen,a\* Wenbo Chen,a Ping Wang,b DZhangjun Fei,a Gary W. Blissarda

ABSTRACT The baculovirus Autographa californica multiple nucleopolyhedrovirus (AcMNPV) is a large double-stranded DNA (dsDNA) virus that encodes approximately 156 genes and is highly pathogenic to a variety of larval lepidopteran insects in nature. Oral infection of larval midgut cells is initiated by the occlusion-derived virus (ODV), while secondary infection of other tissues is mediated by the budded virus (BV). Global viral gene expression has been studied in detail in BV-infected cell cultures, but studies of ODV infection in the larval midgut are limited. In this study, we examined expression of the ~156 AcMNPV genes in Trichoplusia ni midgut tissue using a transcriptomic approach. We analyzed expression profiles of viral genes in the midgut and compared them with profiles from a T. ni cell line (Tnms42). Several viral genes (p6.9, orf76, orf75, pp31, Ac-bro, odv-e25, and odv-ec27) had high expression levels in the midgut throughout the infection. Also, the expression of genes associated with occlusion bodies (polh and p10) appeared to be delayed in the midgut in comparison with the cell line. Comparisons of viral gene expression profiles revealed remarkable similarities between the midgut and cell line for most genes, although substantial differences were observed for some viral genes. These included genes associated with high level BV production (fp-25k), acceleration of systemic infection (vfgf), and enhancement of viral movement (arif-1/orf20). These differential expression patterns appear to represent specific adaptations for virus infection and transmission through the polarized cells of the lepidopteran midgut.

**IMPORTANCE** Baculoviruses such as AcMNPV are pathogens that are natural regulators of certain insect populations. Baculovirus infections are biphasic, with a primary phase initiated by oral infection of midgut epithelial cells by occlusion-derived virus (ODV) virions and a secondary phase in which other tissues are infected by budded-virus (BV) virions. While AcMNPV infections in cultured cells have been studied extensively, comparatively little is known regarding primary infection in the midgut. In these studies, we identified gene expression patterns associated with ODV-mediated infection of the midgut in *Trichoplusia ni* and compared those results with prior results from BV-infected cultured cells, which simulate secondary infection. These studies provide a detailed analysis of viral gene expression patterns in the midgut, which likely represent specific viral strategies to (i) overcome or avoid host defenses in the gut and (ii) rapidly move infection from the midgut, into the hemocoel to facilitate systemic infection.

**KEYWORDS** baculovirus, AcMNPV, insect lepidopteran midgut, *Trichoplusia ni*, Tnms42, transcriptome

aculoviruses are a large group of arthropod-specific viruses with circular double-stranded DNA genomes. Baculovirus genomes range from approximately 80 to 180 kbp and are packaged in rod-shaped nucleocapsids that are enveloped (1, 2). Autog-

Received 24 July 2018 Accepted 16 August 2018

Accepted manuscript posted online 12 September 2018

Citation Shrestha A, Bao K, Chen Y-R, Chen W, Wang P, Fei Z, Blissard GW. 2018. Global analysis of baculovirus Autographa californica multiple nucleopolyhedrovirus gene expression in the midgut of the lepidopteran host *Trichoplusia ni*. J Virol 92:e01277-18. https://doi.org/10.1128/JM.01277-18.

**Editor** Joanna L. Shisler, University of Illinois at Urbana Champaign

**Copyright** © 2018 American Society for Microbiology. **All Rights Reserved.** 

Address correspondence to Gary W. Blissard, gwb1@cornell.edu.

\* Present address: Yun-Ru Chen, National Taiwan University, Taipei City, Taiwan.

<sup>&</sup>lt;sup>a</sup>Boyce Thompson Institute at Cornell University, Ithaca, New York, USA

<sup>&</sup>lt;sup>b</sup>Department of Entomology, Cornell University, New York State Agriculture Experiment Station, Geneva, New York, USA

rapha californica multiple nucleopolyhedrovirus (AcMNPV) has a genome of 133.9 kbp with approximately 156 predicted genes (ORFs) (3). Because the large DNA genome of AcmNPV can be easily engineered for high-level heterologous protein expression, recombinant baculoviruses have been widely used for foreign protein production in many research and biotechnological applications, as well as for production of therapeutics and vaccines (4-6). Baculoviruses are often highly pathogenic to insect larvae. Most baculovirus infections have been described from agriculturally important lepidopteran insect species, although baculoviruses have also been found to infect hymenopteran and dipteran hosts (7, 8). A number of baculoviruses have been used as host-specific biological insecticides in agriculture and forestry (9-11). In nature, baculoviruses are transmitted orally when insect hosts feed on plants contaminated with the virus. Unlike most other viruses, baculoviruses produce two distinct morphological forms (phenotypes) of virions: occlusion-derived viruses (ODV) and budded viruses (BV). ODV, which mediate oral infection, are enveloped virions that are embedded within environmentally stable occlusion bodies (OBs). When released from OBs in the lumen of the insect midgut, ODV initiate infection of the polarized epithelial cells of the midgut. The second form of the virus, BV, is produced when virions bud from the plasma membrane of the cell. Progeny BV bud from the basal surfaces of the polarized midgut cells, circulate in the hemocoel, and mediate systemic spread of the infection among many or most other tissues of the infected host insect (12). Thus, infection of the midgut epithelium by ODV represents the primary phase of the infection, whereas infection of subsequent tissues by BV represents the secondary phase of infection.

The successful infection of the midgut by ODV is a critical event that determines the success of the viral infection in a host, as the midgut represents the first line of cellular defense against baculovirus infection. Following ingestion of OBs, the alkaline environment and proteases present in the midgut lumen cause the crystallized OBs to dissolve or disassemble and release ODV. ODV subsequently pass through the peritrophic membrane (PM), which lines the gut, a process aided by a virus-encoded metalloprotease in at least some baculoviruses (13). ODV bind to apical surfaces on the columnar midgut epithelial cells and enter by membrane fusion at the cell surface (14). Binding and entry of ODV appear to be mediated by a complex of ODV-specific envelope proteins called per os infectivity factors (PIFs) (12, 15-18). Nucleocapsids released into the midgut cell are then transported to the nucleus, where they enter by trafficking through nuclear pores (19, 20). Uncoating of the viral genome is followed by viral early gene transcription, then DNA replication, and late gene transcription (21). The replicated genome is packaged into newly assembled capsids in the nucleus, and the resulting nucleocapsids are then trafficked from the nucleus to the basal membrane regions of the polarized midgut cells, where they bud into the hemocoel to form BV. Also, some nucleocapsids remain in the nucleus, where they are enveloped and become occluded into occlusion bodies. Following infection of midgut cells, secondary infections are observed in midgut-associated tracheal epithelial cells and hemocytes (22, 23). It was also observed that the virus may move very rapidly through the midgut epithelial cells, using what appears to be an alternative nucleocapsid pass-through mechanism (24), and subsequent studies suggested that early expression of the BV envelope protein (GP64) may enhance or may be required for this pass-through mechanism (25). A factor that also influences systemic infection in insect hosts is the physical barrier of the basal lamina, a noncellular sheet that lies along the hemocoel side of the midgut epithelium. A virus-encoded fibroblast growth factor (encoded by v-fqf) appears to stimulate the remodeling of the basal lamina, a process involving host caspases and matrix metalloproteases (26, 27). Because of the critical nature of virus infection of the midgut, the polarized trafficking that must occur there, and the specific nature of this antiviral barrier, viral gene expression in the midgut might be expected to differ from that in other tissues. In the current studies, we examined AcMNPV global gene expression in the infected Trichoplusia ni midgut and compared expression in the midgut with that in cultured cells.

Studies in cultured cell systems show that the baculovirus infection cycle can be

divided into three conceptual phases: early (prior to DNA replication), late (initiating concurrently or after the initiation of DNA replication), and very late (21). Early genes are transcribed by host RNA polymerase II, and among other products, they encode components required for DNA replication and late gene transcription. Following the initiation of DNA replication, baculovirus late genes are transcribed by a virally encoded RNA polymerase that recognizes late promoters containing the core sequence TAAG (28-32). The very late phase corresponds to the hyperexpression of occlusion body related genes and the virion occlusion process. Very late genes (polyhedrin [polh] and p10) are transcribed at extremely high levels. Successful baculovirus infection involves the highly complex and coordinated expression of the 156 early, late, and very late genes. Some viral genes encode proteins that mediate suppression of cellular antiviral responses such as apoptosis, and others modify host physiology with effects on locomotory behavior and the molting cycle (33-38). Most viral structural proteins are encoded by baculovirus late genes. Following synchronous infection in cultured cells, host cell transcription is reduced, resulting in the presence of mostly virus-encoded mRNAs by 24 h postinfection (p.i.) (28, 39, 40). While genome-wide studies of AcMNPV infection in cultured cells have been reported previously (28, 40), similarly detailed studies in the midgut of a natural insect host of AcMNPV have not been performed. In the current study, we examined the primary phase of the infection by transcriptome analysis of the midgut of T. ni larvae orally infected with AcMNPV ODV. In addition, we also compared global AcMNPV gene expression in ODV-infected T. ni midgut with that from a BV-infected T. ni cell line (Tnms42).

Analysis of viral gene expression in the T. ni midgut and comparisons with viral gene expression in the Tnms42 cell line revealed an overall similarity in the general patterns of gene expression. However, we also identified genes that were differentially regulated between the midgut and the cell line, and these differentially regulated genes included genes that appear to be associated with movement of viral nucleocapsids within cells (arif-1/orf20), modulation of the production of budded viruses (fp-25k), and escape of budded viruses from the midgut into the hemocoel (v-fqf). We propose that the observed differences in viral gene expression in the midgut represent adaptations of the virus for accelerated movement of the infection from the primary site of infection into the secondary sites of infection.

# **RESULTS**

AcMNPV transcription in the T. ni midgut. To first examine the program of AcMNPV gene expression in the T. ni midgut, we analyzed the temporal patterns of AcMNPV mRNA levels in T. ni midgut tissue at various times following viral infection. Developmentally synchronized fifth-instar T. ni larvae were orally infected with AcMNPV OBs, and polyA mRNAs were isolated at 0, 6, 12, 18, 24, 36, 48, and 72 h p.i. and then subjected to strand-specific RNA sequencing (RNA-seq). Expression of each viral gene was analyzed (with adjustments for overlapping transcripts) as described previously (28) (see Table S1 in the supplemental material). Unlike synchronous infections of cultured cells with BV, only a subset of the cells in the midgut were infected with the OB inoculum. The reads mapped to each gene, and the total reads mapped to the AcMNPV genome, were used to calculate relative viral gene expression levels as reads per kilobase per million reads (RPKM) values, for each replicate at each time point from 18 to 72 h p.i. (Tables S2 and S3). As the counts of mapped viral gene reads from the two earliest times (6 and 12 h p.i.) were very low, statistically insufficient for comparisons as RPKM calculations, normalized raw read counts for those two time points were used to compare viral gene expression among viral genes at those time points (Table S2). In addition, we also examined the expression of each viral gene from time point to time point by calculating the RPKM value but using the total number of reads (cellular plus viral) for RPKM calculations (Table S3).

First, we identified the most highly expressed viral genes at each sampling time. The top 20 most highly expressed viral genes for each time sampled are shown in Fig. 1. Although the numbers of viral reads were very low at 6 h pi, the most abundant

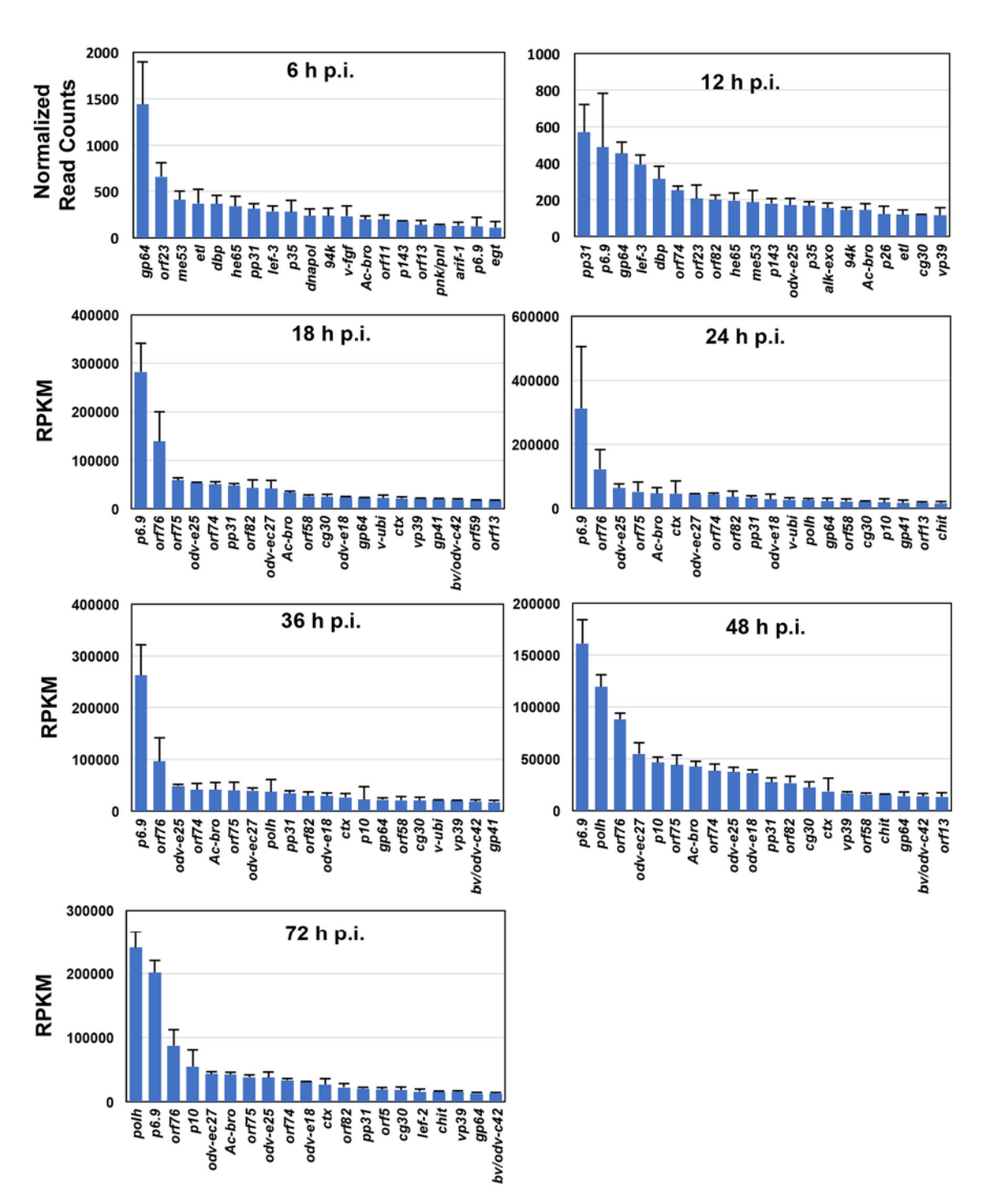
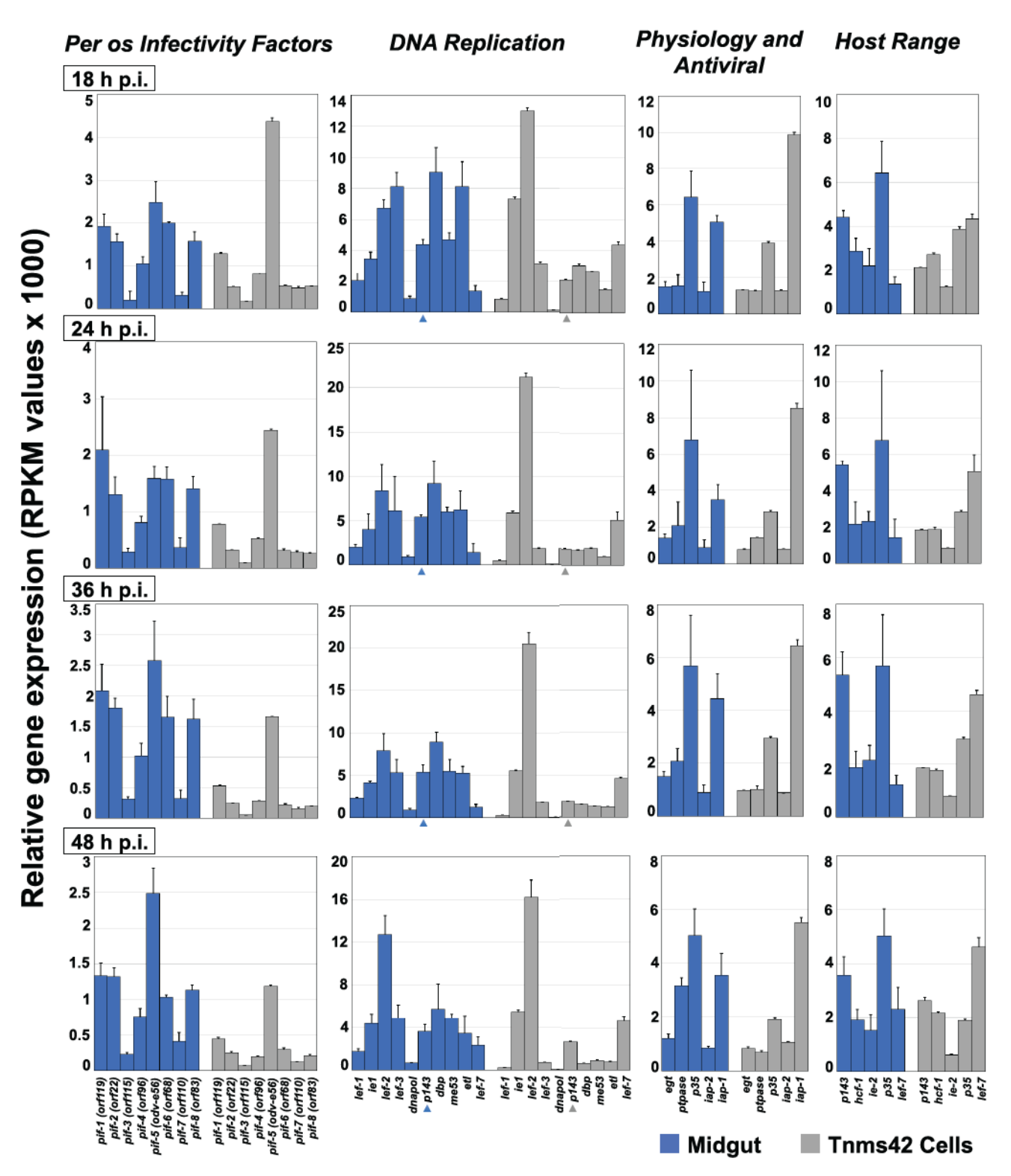


FIG 1 The top 20 most highly expressed AcMNPV genes in T. ni midgut are shown as individual graphs for each time sampled, from 6 h p.i. to 72 h p.i. At 6 and 12 h p.i., highly expressed genes were identified based on normalized read counts that were calculated by dividing the number of mapped viral reads for each gene by the total number of viral reads and multiplying by 10,000. For 18 to 72 h p.i., highly expressed genes were identified based on RPKM values. RPKM values were calculated by standard methods using as a basis the total number of mapped viral reads.

transcript reads detected included those from genes encoding the major BV envelope glycoprotein (GP64), a minor BV envelope protein (Ac23, or F-like protein), early proteins (ME53, ETL, and HE65), DNA-binding proteins (DBP, PP31, and LEF-3), an inhibitor of apoptosis (P35), a helicase protein associated with host range (P143), and a protein that has been associated with BV escape from the midgut (v-FGF). The average number of viral transcript reads detected from midgut tissue increased >10fold between 6 h p.i. and 12 h p.i. (2,665 versus 33,425 viral reads, respectively) (Table S4). By 12 h p.i., the most abundant viral reads were those from genes pp31, p6.9, qp64, lef-3, dbp, orf74, orf23 or ac23, orf82 or tlp, he65, me53, and p143 (Fig. 1; see also Table S2). By 18 h p.i., total viral reads increased to 70,785 (a >2-fold increase from 12 h p.i.) and RPKM values at 18 h p.i. ranged from 65 to 282,398 for 141 viral genes. At 18 h p.i., expression levels of two viral genes associated with BV production (p6.9 and orf76) were dramatically higher than those of other viral genes (Fig. 1, 18 h p.i.). The level of p6.9 transcripts was 4- to 10-fold higher than those of most of the other highly expressed genes at that time. The most highly expressed genes at 18 h p.i. included genes encoding BV structural proteins (qp64, v-ubi, odv-e25, odv-e18, p6.9, vp39, odv-e27, bv/odv-c42, orf58, orf59 or chaB-like, orf75, orf74, pp31, and orf82 or TLP), genes involved in BV egress from the nucleus (gp41, orf75, and orf76), and genes encoding ODV structural proteins (p6.9, ap41, odv-e25, odv-e18, odv-e27, bv/odv-c42, vp39, orf58, orf59 or chaB-like, orf75, orf76, and cg30) (Fig. 1).

At 24 h p.i., the transcript levels of the hyperexpressed very late genes polyhedrin (polh) and p10 were first detected within the top 20 most highly expressed genes. Levels of these hyperexpressed very late genes increased through 72 h p.i. in the T. ni midgut (Fig. 1; see also Table S3, yellow highlight). In contrast, in Tnms42 cells, the expression levels of polh and p10 were substantial by 18 h p.i. and both were among the top 5 most highly expressed viral genes by 24 h p.i (28). In the midgut, polh and p10 transcripts were not among the top 5 most highly expressed AcMNPV genes until 48 h p.i. (Fig. 1). Of particular note, in the T. ni midgut, the p6.9 gene was the most highly expressed gene from 18 to 48 h p.i. and the 2nd most highly expressed gene at 72 h p.i. Other viral genes expressed at relatively high levels from 18 to 72 h p.i. in the midgut were orf74, orf75, orf76, odv-e25, p25, odv-e27, odv-e18, pp31, orf82 or tlp, Ac-bro, cq30, qp64, and ctx as well as vp39 and alk-exo. Viral gene expression in the midgut was substantial by 36 h p.i. and increased further by 48 h p.i., with average viral read counts of 525,255 and 992,388, respectively, at these times (Table S4). By 72 h p.i., polh was the most highly expressed gene, with an RPKM value of 240,697. Expression of the p6.9 gene also remained exceptionally high through later time points, similar to observations in the Tnms42 cell line (28). In addition to polh, mRNAs of genes such as lef-2, ptpase, v-cath, pp34, and the per os infectivity factor (PIF) complex-associated gene (orf5) also reached their highest levels at 72 h p.i. By 72 h p.i., many of the most abundant transcripts represented genes associated with either the BV or ODV (p6.9, odv-ec27, odv-e25, p25, odv-e18, bv/odv-c42, odv-e56, odv-e66, orf119 or pif-1, orf22 or pif-2, orf83 or VP91 or pif-8, orf145, orf75, orf74, qp41, orf58, alk-exo, orf5, and cq30) or the occlusion process (polh, p10, pp34, orf76, orf75, and orf93). Of particular note from the examination of highly expressed genes across all time points in the midgut is the observation that proteins associated with BV production or BV structure are highly represented.

Expression patterns of functionally related AcMNPV genes. We next examined relative expression patterns of several groups of functionally related AcMNPV genes. For this analysis, we compared the expression pattern of each group of genes in the midgut, with the patterns from the same group of genes expressed in the Tnms42 cell line (28) (Fig. 2). Functional gene groups that were examined included viral genes associated with PIFs, DNA replication, host physiological and antiviral responses, host range determination, transcription activators, and structural proteins specific to BV or ODV (21). RPKM values for viral genes were calculated using the total number of viral reads at each time point (Table S2), and thus, expression (RPKM) values are comparable to those for other viral genes examined at the same time point. In Fig. 2, each horizontal group of graphs shows comparisons of midgut and cell line expression patterns (blue versus gray bars) from each set of genes at one time point (18, 24, 36, or 48 h p.i.). In most cases, the patterns of gene expression among the selected groups of genes were generally similar in the T. ni midgut and the Tnms42 cells (Fig. 2, compare blue versus gray bars within each panel). For example, among the pif genes, pif-5 is typically the most abundantly expressed and pif-3 is the least highly expressed gene at each time



**FIG 2** Expression patterns for groups of AcMNPV genes (based on functional groups indicated at the top) are shown as bar graphs, with individual gene names listed at the bottom. Expression levels of each gene at each time point in the *T. ni* midgut are indicated by blue bars, and expression levels in the Tnms42 cell line are indicated by gray bars. Each horizontal group of panels shows comparisons of the expression patterns from sets of genes at a selected time point (18, 24, 36, or 48 h p.i.).

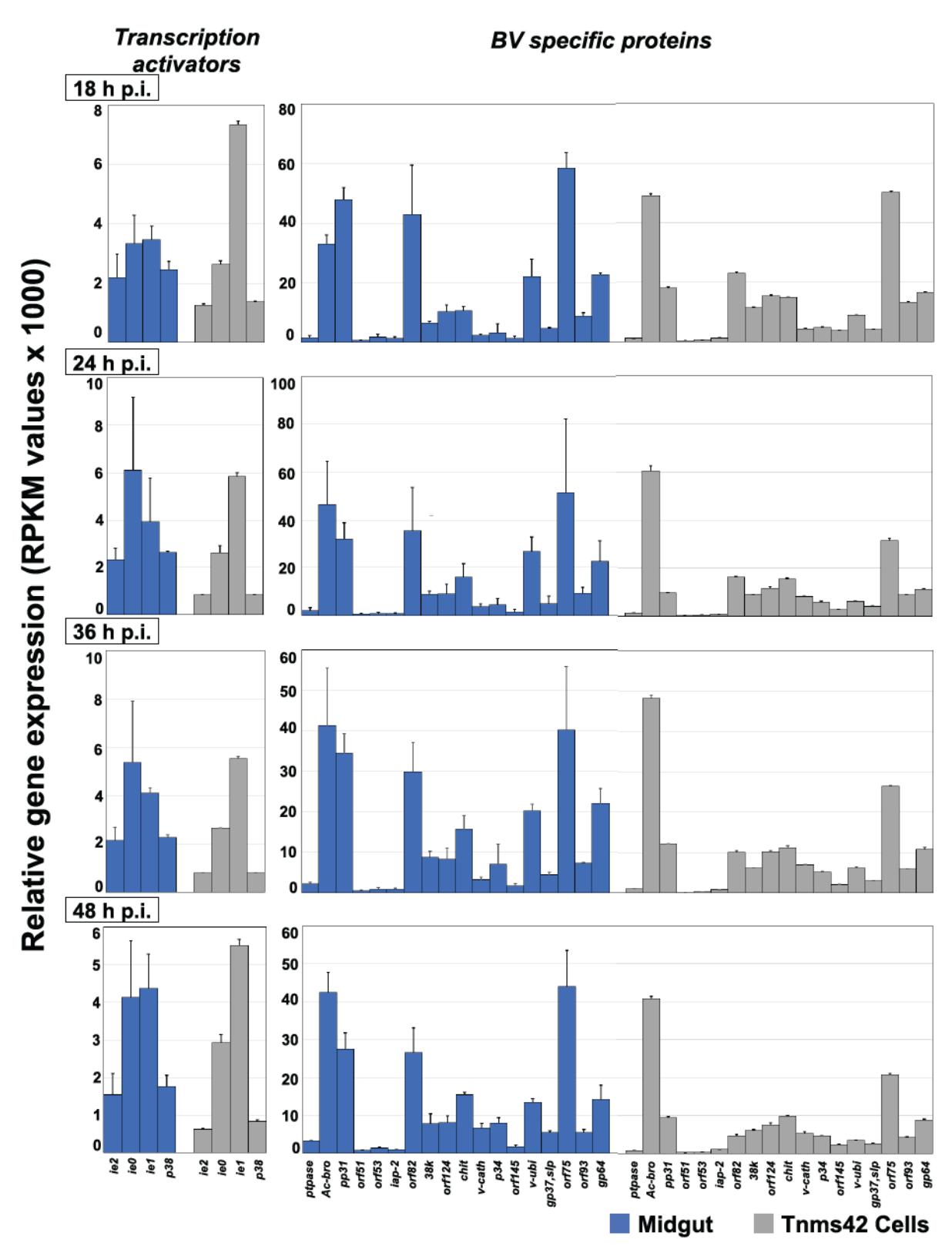


FIG 2 (Continued)

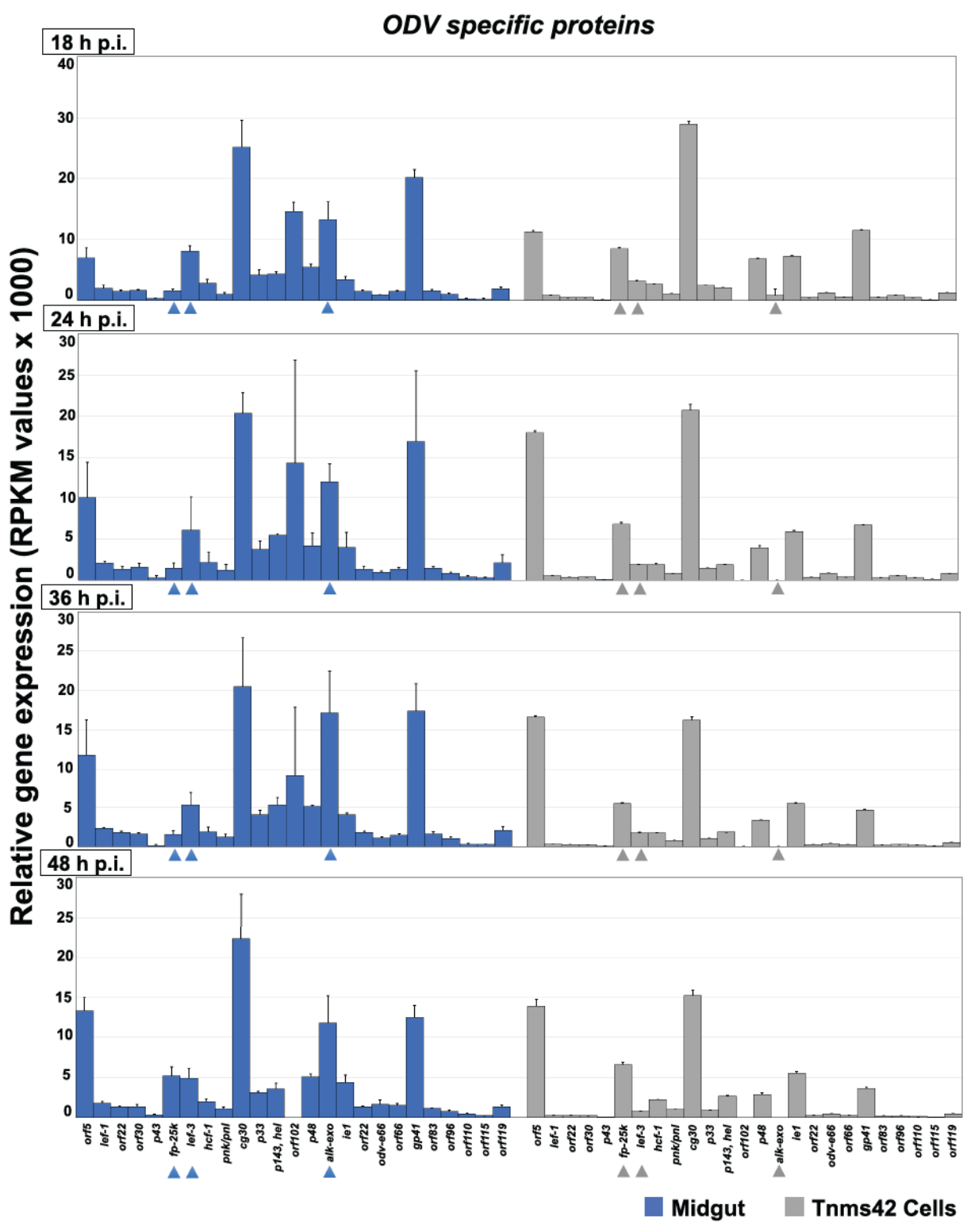


FIG 2 (Continued)

point in both the midgut and in the cell line. (Note that pif-0 [p74] was not included, as the RPKM could not be calculated in the midgut and the cell line). Despite similarities in the patterns of gene expression among the selected groups of genes, we identified three notable exceptions to these general observations. These included the genes fp-25k, lef-3, and alk-exo (Fig. 2, last panel, blue and gray arrowheads). At most time points (18 to 36 h p.i.), transcript levels of fp-25k were relatively low in the midgut, compared with moderate to relatively high levels in the cell line. In contrast, transcripts from lef-3 and alkaline exonuclease (alk-exo) were relatively high in the midgut but comparatively low in the cell line (Fig. 2, last panel). These genes were all found within the group of genes identified as associated with ODV in prior studies (21, 41, 42), although lef-3 and alk-exo are also associated with viral DNA replication (43-45) and may have other roles. The observed differences suggest the possibility of a different pattern of DNA replication and perhaps virion production in the midgut cells from that in cultured cells. In cell culture studies, it was previously observed that viruses with modified forms or deletion of the fp-25k gene had two important phenotypes: (i) lower levels of occlusion bodies were produced (the so-called "few polyhedra" phenotype) (46, 47) and (ii) BV production was substantially increased (47, 48). Reduced expression of fp-25k in the midgut cells may therefore represent differential viral regulation in the midgut that results in enhanced BV production for more rapid movement of the infection out of the midgut for establishing systemic infection.

Comparisons of the expression patterns in Fig. 2 also indicate that *lef-3* and *alk-exo* were both expressed at substantial levels in the midgut. The *lef-3* gene encodes a single-stranded DNA-binding protein that was originally identified as one of the six genes critical for viral origin-dependent DNA replication (49–51). *alk-exo* is an essential AcMNPV gene that encodes an alkaline nuclease that has been proposed to be involved in maturation of Okazaki fragments generated during viral DNA replication (45, 52–54). Interestingly, prior study has shown that the LEF-3 and ALK-EXO proteins interact with each other in infected cells (45). While both are detected in ODV preparations, it is perhaps more significant that they both play important roles in DNA replication. The ALK-EXO protein may also be necessary for recombination. The LEF-3 protein also interacts with the viral DNA helicase encoded by *p143* (44), and somewhat higher midgut levels of *p143* are also suggested by the patterns shown in Fig. 2 (first panel, DNA replication, arrowheads).

Cluster analysis of AcMNPV gene expression patterns in the T. ni midgut. To evaluate overall expression patterns of AcMNPV genes in the T. ni midgut, we also applied a hierarchical cluster analysis (using Euclidean distance metrics and the DESeg2 package). For each gene, we first normalized the read counts (log<sub>2</sub> transformed) and then averaged the read counts from three replicates for each infection time point. We then performed cluster analysis on the averaged normalized reads of viral genes from 18 h p.i. to 72 h p.i. The cluster analysis generated four major clusters of viral genes which we arbitrarily refer to as groups G1, G2, G3, and G4 (Fig. S1 and Table S5). Cluster G1 is comprised of 33 genes, cluster G2 contains 24 genes, cluster G3 contains 30 genes, and cluster G4 contains 69 genes (Table S4). Clusters G2 and G4 contained viral genes with very high expression levels, including polh, p6.9, Ac-bro, odv-e25, alk-exo, orf74, lef-2, p10, v-cath, ptpase, fp-25k, dbp, lef-3, orf-5, and pk-1. Of these, transcript levels of polh, Ac-bro, alk-exo, p10, lef-2, v-cath, ptpase, fp-25k, orf-5, and pk-1 increased from 18 h p.i. to 48 h p.i. Among the four clusters, G1 consisted of genes with the lowest expression levels. Example of genes in the cluster G1 included orf60, orf107, orf121, and orf140. Overall, cluster analysis identified groups of genes with different overall expression levels, and each cluster contains genes with a variety of different patterns of expression from 18 to 72 h p.i.

Comparison of expression patterns of AcMNPV genes in the midgut and cell line. Because of the substantial differences in the midgut and cell line experiments (ODV-mediated oral infection versus BV-mediated synchronous cell line infection), direct comparisons of viral gene expression levels were difficult. Therefore, we used a

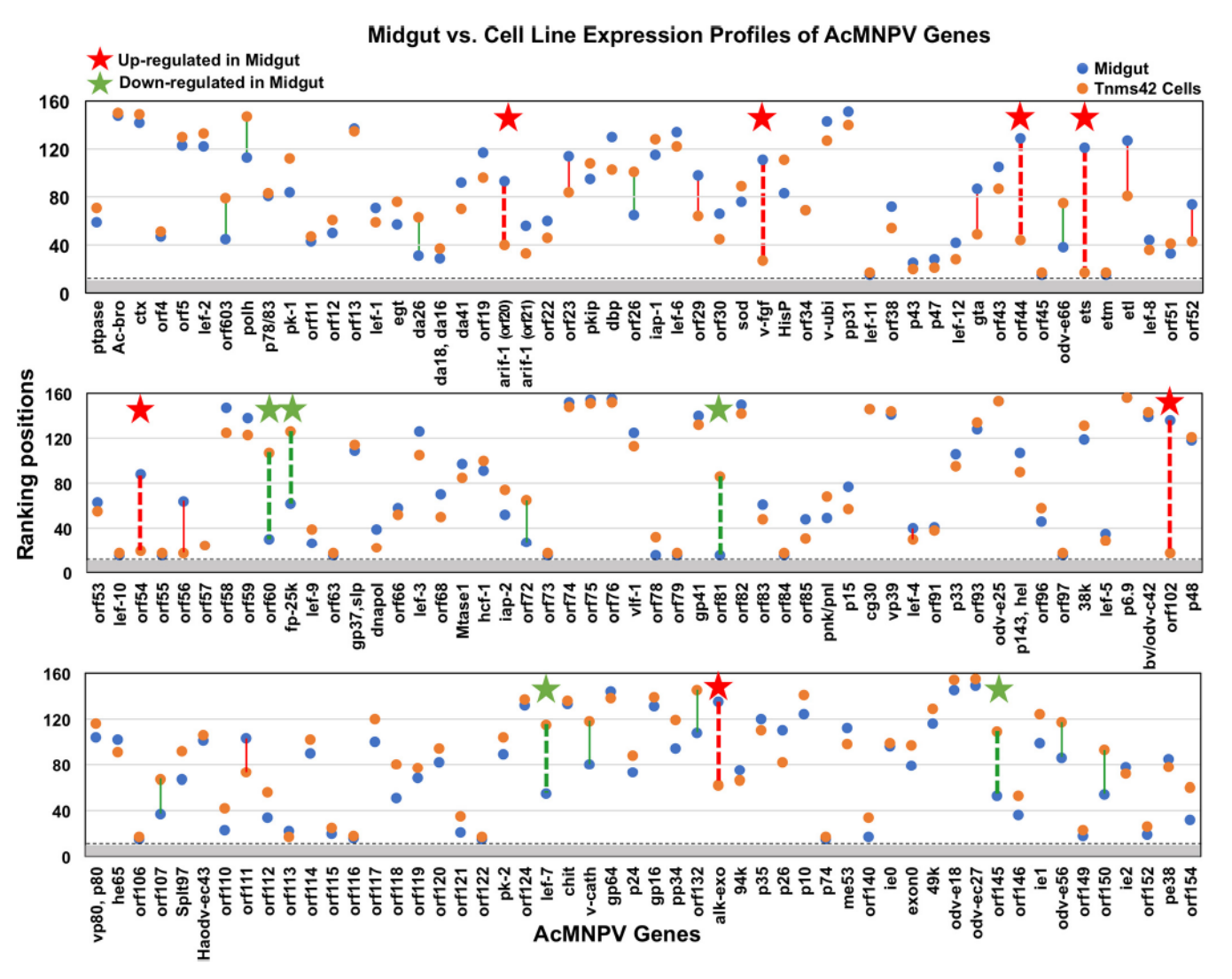


**FIG 3** Comparisons of ranking positions of each of the AcMNPV genes in the *T. ni* midgut and the Tnms42 cell line at 18 h p.i. Based on RPKM values, each gene was ranked in comparison to the expression of all other viral genes at the same time point. The ranking position of each gene expressed in the midgut (blue data points) was compared with that of each gene expressed in the Tnms42 cell line (orange data points). Gene names are indicated on the *x* axis. The horizontal dashed line and gray area represent the number of viral genes for which expression was not detected. Red stars indicate genes with rank positions dramatically higher in the midgut, while green stars indicate genes with rank positions dramatically lower in the midgut, than rank positions in the Tnms42 cell line.

ranking method to compare the expression of viral genes in the midgut and cell line. Based on RPKM values, we ranked the expression level of each gene in comparison to all other viral genes in the same sample (midgut or cell line) at each time point. Each gene was ranked from 1 (lowest expression level) to 156 (highest expression level). We then compared the ranked position of each gene expressed in the midgut with that gene's ranked position from the cell line infection. Comparisons of these ranked expression profiles in the midgut and the cell line demonstrated that the ranking positions of most viral genes were very similar in the midgut and the cell line throughout the infection (Fig. 3; see also Table S6). However, expression of several genes differed substantially (by ≥30 ranking positions) between the midgut and the cell line. A total of 26 genes had differences of ≥30 ranking positions for midgut and the cell line expression at 18 h p.i. Similar numbers of genes were identified at 24 h p.i. (31 genes), 36 h p.i. (30 genes), and 48 h p.i. (26 genes) (Table 1). Also, because comparisons of gene expression under these two experimental conditions (midgut versus cell line) are likely most relevant at the earlier times, we focused on 18 h p.i., the earliest time point with substantial viral gene expression levels in the midgut. We

**TABLE 1** AcMNPV genes with significantly different ranking positions ( $\geq$ 30 ranking positions) between *T. ni* midgut and Tnms42 cells at 18, 24, 36, and 48 h p.i.<sup>a</sup>

Harrie a cont		Ranking		Difference			Ran	king	Difference
Hours post infection	Viral	Tnme42		in rank	Hours post infection	Viral	Tnme42		in rank
	Gene*	Midgut	Cells	position		Gene*	Midgut	Cells	position
	orf603	45	79	-34	36 h p.i.	p78/83	78	38	40
	polh	113	147	-34		orf12	66	104	-38
	da26	31	63	-32		da18, da16	15	55	-40
	orf20, arif-1	93	40	53		orf20, arif-1	96	50	46
	orf23	114	84	30		orf23	110	77	33
	orf26	65	101	-36		dbp	128	95	33
	orf29	98	64	34		orf26	48	97	-49
	v-fgf	111 87	27 49	84 38		v-fgf	67 84	36 52	31 32
	gta orf44	129	44	85		gta orf44	121	30	91
	odv-e66	38	75	-37		ets	103	18	85
	ets	121	17	104		orf54	94	19	75
	eti	127	81	46		orf60	21	109	-88
	orf52	74	43	31		fp-25k	60	125	-65
	orf54	88	19	69		orf63	15	66	-51
18 h p.i.	orf56	64	17	47		iap-2	40	80	-40
	orf60	30	107	-77		orf72	23	72	-49
	fp-25k	62	126	-64		orf78	15	60	-45
	orf72	27	65	-38		orf81	15	102	-87
	orf81	15	86	-71		orf102	129	18	111
	orf102	136	17	119		orf118	36	69	-33
	orf107	37	67	-30		lef-7	54	119	-65
	orf111	103	73	30		v-cath	98	132	-34
	lef-7	55	115	-60		orf132	101	142	-41
	v-cath	80	118	-38		alk-exo	136	18	118
	orf132	108	145	-37		p26	111	76	35
	alk-exo	135	62	73		orf140	37	70	-33
	orf145	53	109	-56		orf145	65	108	-43
	odv-e56	86	117	-31		orf150	45	94	-49
	orf150	54	93	-39		orf154	42	96	-54
	pk-1	98	128	-30		p78/83	74	25	49
	orf20, arif-1	91	36	55	48 h p.i.	orf12	92	130	-38
	orf23	113	81	32		egt	54	86	-32
	dbp	129	93	36		da18, da16	21	54	-33
	orf26	53	105	-52		orf23	109	78	31
	iap-1	99	130	-31		dbp	121	71	50
	v-fgf	102	56	46		orf26	63	100	-37
	orf44	106	37	69		v-fgf	82	42	40
	ets	115	18	97		orf38	17	49	-32
	etl	121	76	45		orf44	103	18	85
	orf52	86	52	34		ets	96	18	78
24 h p.i.	orf54	68	25	43		orf54	79	19	60
	orf60	17	108	-91		orf60	41	114	-73
	fp-25k	61	126	-65		orf63	17	62	-45
	orf72	19	68	-49		lef-3	113	79	34
	orf78	14	51	-37		hcf-1	78	109	-31
	orf81	14	82	-68		iap-2	46	93	-47
	orf91	85	55	30		orf72	26	89	-63
	orf102	134	18	116		orf81	17	99	-82
	he65	108	78	30		pnk/pnl	52	92	-40
	orf107	37	77	-40		lef-7	85	122	-37
	orf118	38	80	-42		alk-exo	131	18	113
	lef-7	60	118	-58		p26	111	74	37
	orf132	104	143	-39		orf140	36	94	-58
	alk-exo	133	18	115		orf145	69	110	-41
	p26	109	79	30		orf150	62	98	-36
	orf140	32	63	-31					
	orf145	67	112	-45					
	odv-e56	65	107	-42					
	orf150	49	98	-49					
	orf154	50	104	-54					

 $a^*$ ,The list includes AcMNPV genes that differed by ≥30 in ranking positions between the midgut and Tnms42 cells. Each gene was ranked against all other viral genes at each time point based on its RPKM value, and the ranking position was compared between the midgut and Tnms42 cells. AcMNPV genes with ranking differences of ≥50 ranking positions are indicated in bold red (genes with higher expression in the midgut) and bold green (genes with higher expression in Tnms42 cells).

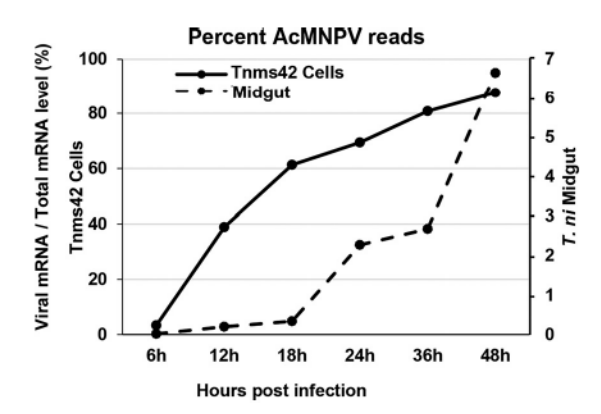


FIG 4 Graph showing AcMNPV mRNA reads as a percentage of total mRNA reads at each time point from 0 to 48 h p.i. The percentages of AcMNPV mRNA reads relative to total mRNA (virus plus host) reads in the infected T. ni midgut are indicated by the dashed line (right y axis). Similarly, the percentages of AcMNPV reads from infected Tnms42 cells are shown as a solid line (left y axis) (data from reference 28).

identified seven genes with ranking position differences of ≥50 at 18 h p.i. and for which expression levels were higher in the midgut than in the cell line: orf20 or arif-1, v-fgf, orf44, ets, orf54, orf102, and alk-exo (Fig. 3, red stars). Further, we identified five genes (with rank position differences of ≥50) with higher expression levels in the cell line than in the midgut at 18 h p.i. These five genes included orf60, fp-25k, orf81, lef-7, and orf145 (Fig. 3, green stars). We also noted that of the 12 genes identified (listed above) at 18 h p.i., the expression profiles of several genes (orf-44, ets, orf60, orf81, and alk-exo) differed substantially between the midgut and cell line at all times from 18 h p.i. to 48 h p.i. (Table 1). Further, expression profiles of fp-25k were significantly lower in the midgut, while orf102 expression levels were higher in the midgut, than in the cell line from 18 h p.i. to 36 h p.i. A few genes, such as v-fgf, orf23 or Ac23, and orf54 or vp1054, were consistently highly expressed (differences of ≥30 rank positions) in the midgut. In addition, transcript levels of genes orf26, orf72, lef-7, orf145, and orf150 were consistently found at low levels in the midgut compared with the cell line (Table 1).

Correlation analysis of viral expression patterns in midgut and cell line. In these and prior experiments, the percentage of T. ni midgut cells infected by viral OBs is substantially lower than the percentage of cultured cells infected by BV (approximately 10 to 30% versus 100%, respectively). In the current studies, we used a recombinant AcMNPV containing an mCherry marker gene to titrate the OB dose and selected the lowest OB dose (7  $\times$  10<sup>4</sup> OBs/larva) that resulted in the maximal apparent percentage of infected midgut cells in newly molted 5th-instar larvae. We estimated an infection rate of approximately 10 to 30% of the midgut cells, and higher rates of infection were not observed with increased doses of OBs. A prior study reported variable results from infections of starved (but not synchronized) 4th-instar T. ni larvae using a dose of 1  $\times$ 10<sup>4</sup> AcMNPV OBs, although percentages of infected cells were not estimated (55). A comparison of total viral reads in the midgut and the cell line at various times postinfection highlights the lower rate of infection in the midgut (Fig. 4), even at high doses of OBs. In synchronously infected Tnms42 cells, we previously observed that RNA-Seq reads from viral transcripts increased to >80% of total reads by 48 h p.i (28). In contrast, in the midgut we found that the percentage of viral reads increased to <7%by 48 h p.i. (Fig. 4). When analyzing the expression of individual viral genes in the midgut and cell line at parallel time points, we found that the pattern of gene expression for most viral genes in the midgut was, in most cases, very similar to that in the cell line (Fig. 2 and 3), although for a limited number of transcripts, expression patterns were substantially different in the midgut and cultured cells. Because our analysis compares different types of infection (ODV- versus BV-mediated infections) in two different cell systems, we asked whether the viral program of expression was the same or could be time shifted or offset in the midgut and cell line. To address this

question, we performed a correlation analysis on the patterns of viral gene expression in the midgut and the Tnms42 cell line. The pattern of midgut expression of each gene was compared with the pattern of expression from the same gene in the Tnms42 cell line, and a correlation value was calculated as described in Materials and Methods (Table 2). We performed a pattern correlation analysis between the midgut and the cell line using three sets of infection timelines: analysis 1, midgut at 18 to 48 h p.i. versus cell line at 6 to 24 h p.i.; analysis 2, midgut at 18 to 48 h p.i. versus cell line at 12 to 36 h p.i.; and analysis 3, midgut at 18 to 48 h p.i. versus cell line at 18 to 48 h p.i. Correlation coefficient (R) values ranged from -1 (negatively correlated) to +1 (positively correlated) (Table 2). Analysis 2 resulted in the greatest number of genes with a positive correlation (R > 0.1) (98 genes), as well as the highest sum, median, and mean values. Figure S2 shows several examples of gene expression patterns that have higher correlation values when timelines are shifted as in analysis 2 (Fig. S2, Tnms42 cells, -6 h). Thus, based on this analysis it appears that the expression pattern of AcMNPV genes in the midgut is slightly shifted, with the highest correlation resulting from the comparison of midgut (18 to 48 h p.i.) versus cell line (12 to 36 h p.i.).

While the expression patterns of the large majority of viral genes were positively correlated in midgut versus cell line comparisons in analysis 2, we are especially interested in genes that may be uniquely regulated in the midgut (i.e., negatively correlated). In analysis 2 (which showed the highest positive correlation), we identified 39 genes with expression patterns that were negatively correlated. Among these 39 genes, 22 were strongly negatively correlated, with R values between -0.5 and -1 (Table 2, pink highlight). Graphic examples of the expression patterns for a few genes with strong negative correlations between the midgut and the cell line are shown in Fig. 5 (ptpase, HisP, odv-e66, p24, qp16, 49k, odv-e18, and da26).

## DISCUSSION

Baculoviruses produce two virion phenotypes with distinct roles in the infection cycle in nature. Primary infection is initiated by ODV and occurs in the polarized epithelial cells of the midgut, whereas secondary infection is initiated by BV and occurs in other tissues after the virus escapes the primary midgut infection (12, 21, 56). Because the insect midgut is highly adapted to insults and assaults from a variety of pathogens, baculovirus infection in the midgut might be expected to differ from infection in other tissues. In this study, we first examined global AcMNPV gene expression in the midqut at different time points of the infection, and then we compared patterns of baculovirus gene expression between ODV-infected midgut cells and BV-infected cultured cells of the same species. The virus faces unique challenges in terms of successfully infecting and then exiting from the midgut. These include physical factors, such as the peritrophic matrix that lines the gut on the apical side of the midgut epithelium, the polarized architecture of midgut epithelial cells, and the basal lamina that separates midgut cells from the hemocoel. Also, defensive reactions of insect midgut cells appear to be adapted for detection of microbes and for subsequent triggering of antimicrobial responses such as cell loss (sloughing) (25, 57, 58). Thus, because the virus encounters unique challenges during the primary phase of infection, it is perhaps not surprising that we observed specific differences in viral gene expression in the midgut compared with that from cultured cells (which likely simulates the secondary phase of infection).

Because antiviral responses of infected lepidopteran midgut epithelial cells are likely to be robust, rapid virus replication, BV production, and egress from midgut cells may be imperative for establishing successful infection of the animal. Viral genes that were highly expressed in the midgut suggest that BV production and egress may be prioritized over OB production in the midgut. We found that the following viral genes were consistently expressed at high or moderately high levels in the midgut throughout the 72-h sampling period following oral infection (Fig. 1; see also Table S2): p6.9, pp31, gp64, Ac-bro, orf13, orf124, odv-e25, bv/odv-c42, orf82, orf74, orf75, orf76, alk-exo, vp39, gp41, cg30, dbp, and lef-6. A number of these genes encode structural proteins

TABLE 2 Correlation analysis of viral gene expression patterns between midgut and Tnms42 cells

	Pearson correlation coefficient ( R )					
	Analysis 1	Analysis 2	Analysis 3			
March Comm.	Midgut (18-48 h p.i.) vs. Tnms42 Cells (6-24 h p.i.)	Midgut (18-48 h p.i.) vs. Tnms42 Cells (12-36 h p.i.)	Midgut (18-48 h p.i.) vs. Tnms42 Cells (18-48 h p.i.			
Viral Gene ptpase	-0.57	-0.94	-0.8			
Ac-bro	0.52	0.69	0.3			
ctx	-0.12	0.38	0.8			
orf4 orf5	0.03	0.44 0.88	0.0			
lef-2	0.80	0.59	0.0			
orf603	0.33	0.60	0.1			
polh	0.98	0.87	0.8			
p78/83, orf1629 pk-1	-0.42 0.96	0.50 0.50	0.6			
orf11	-0.05	0.37	0.2			
orf12	-0.30	0.87	0.0			
orf13	-0.16	0.98	0.7			
ef-1 egt	0.08	0.14	0.0			
da26	-0.91	-0.75	-0.2			
da18, da16	-0.67	0.88	0.5			
da41	0.68	0.87	0.			
orf19 orf20	-0.28 0.57	-0.09 0.50	9.0 -0.4			
arif-1	0.57	0.50	-0.			
orf22	0.14	-0.08	0.0			
orf23	0.74	0.86	0.7			
okip	-0.69	-0.74	0.0			
ibp orf26	0.37 -0.86	0.46 -0.09	0.			
ap-1	-0.61	0.58	0.			
of-6	0.79	0.81	0.			
orf29	0.95	0.91	0.			
orf30 ood	0.71 0.27	0.78 0.68	0.			
-fgf	0.88	0.66	0.			
lisP	0.79	-0.83	-0.			
rf34	0.30	-0.27	-0.			
-ubi	0.09	0.81	0.			
p31 ef-11	0.95	0.85	0.			
orf38	-0.46	0.79	0.			
143	0.51	0.51	0.			
47	-0.14	-0.07	-0.			
ef-12	-0.16	-0.36	-0.			
rf43	0.56 0.11	0.67 0.19	0.			
orf44	0.80	0.83	0.			
orf45	0.00	0.00	0.			
dv-e66	0.19	-0.91	-0.			
ts tm	0.00	0.00	0.			
eti	0.84	0.82	0.			
ef-8	-0.57	0.24	0.			
orf51	-0.39	-0.26	0.			
orf52	0.31	0.68	-0.			
ef-10	-0.97 0.00	0.52	0.			
er-10 erf54	-0.16	0.29	-0.			
orf55	0.00	0.00	0.			
orf56	0.95	0.00	0.			
orf57	0.11 -0.61	0.29	-0.			
orf58 orf59	-0.61 -0.68	0.60	0.			
orf60	-0.48	-0.56	0.			
p-25k	0.22	-0.74	-0.			
of-9	-0.11	0.69	0.			
rf63 p37,slp	0.00	0.00 -0.64	0. -0.			
Inapol	0.37	0.42	0.			
rf66	-0.89	-0.10	0.			
of-3	0.96	0.99	0.			
rf68	-0.30	0.84	0.			
Mtase1 ncf-1	-0.42 0.97	0.55 0.92	-0. 0.			
ap-2	0.34	0.63	0.			
orf72	0.67	0.68	0.			
orf73	0.00	0.00	0.0			
orf74	-0.84	0.61	0.			
orf75 orf76	-0.63 -0.56	0.93 0.97	0.			
rtro	-0.39	0.80	0.			
orf78	0.00	0.00	0.0			

orf79	0.00	0.00	0.00
gp41	-0.29	0.83	0.84
orf81 orf82	0.00 1.00	0.00 1.00	0.00
orf83	0.27	0.53	0.44
orf84	0.00	0.00	0.00
orf85	0.97	0.23	0.25
pnk/pnl	-0.49	-0.30	-0.97
p15	0.76	0.89	0.93
cg30	-0.99	0.46	0.74
vp39 lef-4	-0.60 0.91	0.22 0.95	0.49 0.84
orf91	0.76	-0.04	0.06
p33	-0.18	0.70	0.70
orf93	0.02	0.92	0.78
odv-e25, p25	0.00	0.98	0.66
p143, hel	-0.09	-0.06	-0.98
orf96 orf97	-0.36 0.00	0.61	0.55
38k	0.88	0.61	-0.66
lef-5	0.26	0.59	0.56
p6.9	0.03	0.76	0.59
bv/odv-c42	-0.19	0.54	0.65
orf102	0.00	0.00	0.00
p48 vp80, p80	-0.80 -0.70	-0.03 0.86	0.45 0.96
vp80, p80 he65	-0.70	0.86	0.62
orf106	0.00	0.00	0.00
orf107	-0.20	0.92	0.97
Spit97	0.80	-0.35	-0.79
Haodv-ec43	-0.64	-0.12	0.09
orf110	0.42	-0.57	-0.71
orf111 orf112	0.89 0.64	0.85 0.32	1.00 0.21
orf113	-0.03	0.00	0.00
orf114	-1.00	0.16	0.45
orf115	0.64	-0.31	-0.61
orf116	0.44	0.76	-0.71
orf117	0.14	0.98	0.87
orf118 orf119	0.98 0.53	0.97 0.65	0.81
orf120	-0.99	0.42	0.52
orf121	-0.81	0.68	0.96
orf122	0.00	0.00	0.00
pk-2	-0.39	0.47	-0.32
orf124	-0.06	0.96	0.94
lef-7 chit	0.57 0.93	0.14 0.64	-0.01 -0.40
v-cath	0.89	0.54	-0.40
gp64	0.76	0.60	0.66
p24	0.33	-0.94	-0.76
gp16	0.07	-0.93	-0.69
pp34	0.84	0.76	-0.32
orf132 alk-exo	-0.08 -0.05	-0.74 -0.28	-0.44 -0.06
94k	-0.05	-0.28	-0.06
p35	0.40	0.87	0.69
p26	0.34	0.34	0.26
p10	0.94	0.97	0.88
p74	0.00	0.00	0.00
me53 orf140	-0.52 0.29	0.11	-0.14
le0	0.29	0.77 -0.77	0.76
exon0	0.90	-0.64	-0.85
49k	0.08	-0.97	-0.70
odv-e18	0.65	-0.77	-0.91
odv-ec27	0.18	-0.82	-0.57
orf145 orf146	0.96	-0.69	-0.93 -0.55
orf146 le1	-0.14 -0.92	-0.52 -0.97	-0.55 -0.93
odv-e56	-0.59	-0.40	-0.06
orf149	-0.45	0.36	-0.74
orf150	-0.43	-0.70	-0.08
ie2	0.50	0.55	0.60
orf152	-0.93	-0.97	0.30
pe38 orf154	0.41 0.93	0.64	0.30
Sum	0.93	43	32
Median	0.05	0.44	0.25
Mean	0.12	0.27	0.20
	3.12	3.21	

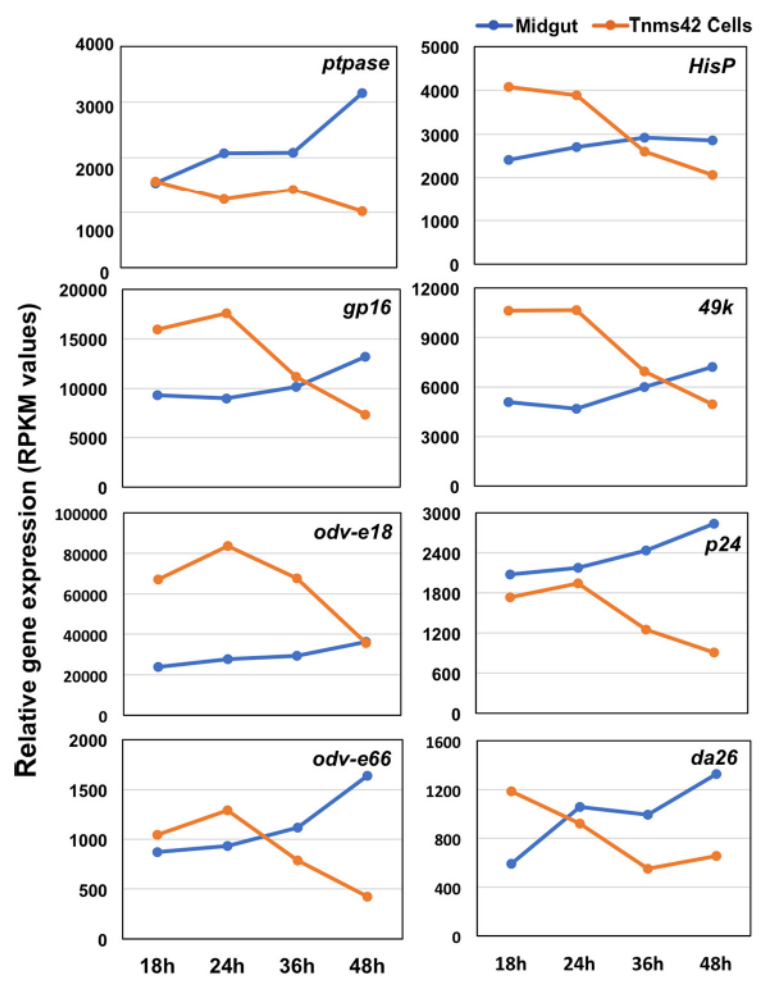


**FIG 5** Expression patterns of a variety of AcMNPV genes with strong negative correlations between midgut and cell line expression. The expression pattern of each gene in the *T. ni* midgut and the Tnms42 cell line was examined by correlation analysis, and Pearson's correlation coefficient (*R*) was calculated for each gene. Correlation analysis was performed on the expression pattern of each gene in the midgut (18 to 48 h p.i.) compared with the expression pattern of the same gene in the Tnms42 cell line at three different time lines (Table 2). The strongest overall positive correlations were between the midgut at 18 to 48 h p.i. and Tnms42 cells at 12 to 36 h p.i. However, several genes had strong negative correlations at these times, and they are illustrated here and highlighted in Table 2 (analysis 2).

associated with nucleocapsids or BV, and others have been identified as important or essential for efficient BV production (gp64, p6.9, vp39, pp31, odv-e25, odv-e18, orf74, orf75, orf82, alk-exo, and possibly gp41 and lef-6) (12, 21). In addition to roles in BV production, genes such as Ac-bro (Ac-2) may play a role in escape from the midgut. A Bombyx mori nucleopolyhedrovirus (BmNPV) homolog of the Ac-Bro protein (BmNPV Bro-A) was previously shown to interact with Bombyx mori laminin, a component of the basal lamina (59). Thus, highly expressed Ac-Bro in midgut cells may aid in disruption or reorganization of laminin surrounding the midgut, facilitating release of BV. Overall, the relatively high early levels and continued midgut expression of these viral genes suggest a program of expression that favors BV production and escape from the midgut.

Because infections in the midgut and cell line differed in terms of relative infection levels (Fig. 4), we used two complementary approaches to compare the patterns of viral gene expression. First, we compared patterns of gene expression within functional sets of viral genes (Fig. 2). Second, we used a ranking approach to compare each gene's expression in the context of all other viral genes, comparing each gene in the midgut and cell line at a particular time point (Fig. 3). In these comparisons, we focused on

genes with substantial differences in expression patterns in the midgut versus the T. ni cell line. Within functional groups of genes, we identified several genes that differed in their expression patterns in midgut and cell line studies. These genes included p35, which had higher relative expression in the midgut, and lef-7 and fp-25k, which were expressed at lower relative levels in the midgut. Using the second method for ranking gene expression across the viral genome (Fig. 3), we focused on the analysis at 18 h p.i., the earliest time point when viral transcripts become abundant in the midgut (see also 18 to 72 h p.i. in Tables 1 and S6). We identified 12 viral genes that differed dramatically in midgut and Tnms42 cell line expression at 18 h p.i. (Fig. 3). While the functional roles of some of these genes are not known, the differences observed for several genes are consistent with the concept of enhanced BV production and escape of BV from the infected midgut. Most striking are the differential expression patterns for five genes (orf20 or arif-1, orf102, alk-exo, orf54, and v-fgf) that were expressed at much higher relative levels in the midgut and one gene (fp25k) that was expressed at lower levels in the midgut.

Two of the genes identified above are associated with remodeling of the actin cytoskeleton within infected cells. orf20 (arif-1) encodes a protein that mediates F-actin localization at the plasma membrane early in the infection cycle (60-62). In studies of BmNPV containing a disrupted arif-1 gene, it was reported that viral propagation was delayed in infected B. mori larvae, and it was proposed that arif-1 enhanced systemic infection in larvae (63). orf102 is an essential gene encoding a protein that is required for nuclear actin localization and polymerization, and is required for BV production (64-67). Orf102 is a member of a complex containing viral proteins EC27, C42, and P78/83. Two other genes identified as differentially expressed in the midgut and cell line (alk-exo and orf54) are both required for nucleocapsid assembly and thus are essential for BV production.

Perhaps most striking and informative regarding BV production and midgut escape is the detection of differential expression of v-fqf and fp-25k. The role of the v-fqf gene in facilitating systemic infection has been studied extensively (27, 68-74). The AcMNPV v-fqf gene activates metalloproteases and effector caspases to degrade the basal lamina, which serves as a midgut escape barrier (26, 27). Thus, higher levels of v-fqf expression in the midgut likely facilitate midgut escape and rapid dissemination of the virus infection to secondary tissues. The relative levels of fp-25k were low in the midgut in comparison to that in the cell line. Based on prior studies, a reduced level of the fp-25k gene product suggests lower OB levels (the so-called "few polyhedra" phenotype) (46, 47) and increased BV production (47, 48). Thus, the differential midgut expression of these two genes, fp-25k (which was decreased) and v-fqf (which was increased), suggests a viral gene expression program in the midgut that favors rapid BV production and enhanced escape.

The temporal shift observed in the overall expression pattern of viral genes between the midgut and the cell line may also provide some additional insight into the variation in the viral infection cycle between primary and secondary infections. However, the many variables in the two infection scenarios and experimental systems require caution in any interpretations. It is as yet unclear how a temporal shift in the overall expression pattern, as observed in this study, would increase or decrease success of the virus. It is possible that the observed temporal shift in the expression pattern could result from either important biological factors (such as the different structural features of ODV and BV that initiate infection in primary and secondary infections) or different experimental conditions (midgut infections by ODV versus cultured cell infections by BV). Also, the possible effects of multiplicity of infection (MOI) on experimental results are unclear. T. ni larvae were orally infected with a relatively high dose of OBs (7  $\times$  10<sup>4</sup> OBs per larva). An AcMNPV OB contains many (approximately 10 to 30) ODV virions and each ODV virion contains multiple (approximately 5 to 25) nucleocapsids (75). Thus, while only a subset of midgut cells are infected, those infected midgut cells typically receive many AcMNPV nucleocapsids, which may be equivalent to the higher MOIs used in BV infections (28).

There are many differences between primary and secondary infections, and comparisons are experimentally challenging. In this study, we first examined AcMNPV gene expression in an ODV-initiated infection of T. ni midgut cells and then used several approaches to compare the expression levels of AcMNPV genes in the T. ni midgut and a T. ni cell line. Our results suggest that the differences in the expression of specific genes and general expression patterns represent differences related to efficient viral replication (BV production and budding) and movement through midgut tissue during the primary phase of the infection cycle. To our knowledge, no prior study has carefully examined global baculovirus gene expression in the lepidopteran midgut and compared the patterns of global baculovirus gene expression between ODV-infected midgut cells and BV-infected cultured cells of the same species. The results illuminate differences in viral interactions and activity during the primary and secondary phases of infection. It will be important in future studies to understand the differences resulting from initiation of viral infection by the different virion phenotypes, as well as the effects of different cell or tissue types on the program of viral gene expression. Different viral expression patterns may be associated with specific tissue types in the secondary phase of infection and could represent adaptations for efficient virus propagation or responses to antiviral mechanisms present in specific tissues. In addition to developing a better understanding the overall biology of baculovirus-host interactions, identifying unique viral gene expression profiles in the midgut and other tissues may also aid in the design of recombinant baculoviruses for more effective biological control of target insect pest populations in agriculture and forestry.

#### **MATERIALS AND METHODS**

Insects and viruses. *T. ni* eggs from the Cornell strain, maintained in the Wang laboratory (Cornell University, Geneva, NY), were collected on sheets of wax paper, surface sterilized by immersion in 10% Clorox for 20 min, and then rinsed three times with sterile deionized water. After surface sterilization, egg sheets were air dried for approximately 15 min, cut into pieces containing approximately 30 to 40 eggs each, and then placed in 16-oz cups containing artificial-wheat germ diet. Eggs were maintained in a growth chamber at 27°C with a light-dark photoperiod of 14:10 h. Larvae for experiments were developmentally synchronized in the following manner. Larvae that had ceased feeding at the end of the 4th instar were isolated and held without diet for 0 to 5 h. From that group, newly molted 5th-instar larvae (0 to 5 h old) were selected and fed either a virus-containing or a control solution of sucrose (see below).

To produce wild-type (WT) AcMNPV occlusion bodies (OBs) for this study, WT AcMNPV was purified from a single well by a limiting-dilution assay (4) and amplified; the titer was determined, and then the virus was used to infect *T. ni* cell line Tnms42 (an alphanodavirus-free cell line subcloned from BTI-Tn5B14 cells) (28, 76). Tnms42 cells were infected at an MOI of 0.1 and maintained in TNM-FH medium (77) (Invitrogen) supplemented with 2.5% fetal bovine serum (FBS) at 28°C. After 7 days, OBs were collected and purified by one successive round of vortexing, pelleting, and resuspension in a solution of 0.5% SDS and 0.5 M NaCl, as previously described (4). OBs were then pelleted and resuspended in 10 ml of double-distilled water (ddH<sub>2</sub>O). Similar to the case with WT AcMNPV, we also prepared OBs from a recombinant baculovirus carrying a 2nd copy of the viral capsid protein VP39 fused to 3 copies of a marker gene, mCherry (virus 3mC) (78). The mCherry-labeled virus, 3mC, was used to determine the minimum number of OBs required to obtain maximum midgut cell infection in *T. ni* larvae. Larvae were fed increasing doses of OBs of virus 3mC, and after various incubation times, midguts were dissected and examined by fluorescence microscopy to estimate optimal midgut infection. Based on our observation, we estimate that the maximal infection rate was ~30% of the midgut cells.

For infections, larvae were orally inoculated with wild-type AcMNPV strain E2 by hand feeding 5  $\mu$ l of a 10% sucrose solution containing a total number of 7  $\times$  10<sup>4</sup> OBs of WT AcMNPV (1.4  $\times$  10<sup>4</sup> OBs/ $\mu$ l) using a Gilson P20 pipette. Larvae that failed to consume the entire sucrose solution were discarded. Mock-infected control larvae were fed a 10% sucrose solution containing no virus. At 1 h postfeeding, control or virus-inoculated larvae (approximately 30 each) were placed in cups containing artificial diet and reared in a growth chamber at 27°C (14:10 lightdark) as described above. Midgut tissues were dissected at 0, 6, 12, 18, 24, 36, 48, and 72 h p.i. Dissected midgut tissues were immediately preserved in RNAater RNA stabilization solution (Ambion) on ice and then stored at  $-80^{\circ}$ C until total RNA extraction was performed with TRIzol reagent (Ambion) according to the manufacturer's instructions. For each time point and treatment (infected or control), we generated three replicate samples. Midguts from six larvae were pooled for each replicate. Following total RNA extraction, midgut RNA samples were screened by PCR for a known T. ni tetravirus (P. Wang, unpublished data), a virus that replicates in the T. ni midgut. Only samples that were negative for the T. ni tetravirus were used for experiments.

**RNA-Seq library preparation.** Strand specific RNA-Seq libraries were constructed as described previously (79). Briefly, 3  $\mu$ g of each total RNA was used to isolate poly(A) mRNA using oligo(dT)25 Dynabeads (Invitrogen). The poly(A) mRNA samples were then fragmented at 94°C for 5 min in buffer containing ProtoScript II reaction buffer (New England BioLabs [NEB]), hexamer (Qiagen), and oligo(dT)<sub>23</sub>

VN (NEB). Subsequently, first-strand cDNA was synthesized using ProtoScript II and the RNA/cDNA hybrid was purified with RNA Clean XP (Beckman Coulter). Second-strand synthesis was carried out with a reaction mix consisting of RNase H (NEB), the Klenow fragment of DNA polymerase I (NEB), and deoxynucleoside triphosphate (dNTP) mix with dUTP (dATP, dCTP, dGTP, and dUTP) (Promega Corporation). cDNA fragments were then end repaired and dA tailed before TruSeq universal adapters were ligated. After adapter ligation, the dUTP-containing strand was removed by digestion with uracil DNA glycosylase (NEB), and PCR amplification was performed with library-specific TruSeq PCR primers for 13 cycles. Amplified libraries were purified with AMPure XP beads (Beckman Coulter) and quantified, and 19 libraries were pooled for each lane of sequencing on the Illumina HiSeq4000 platform at the CLC Genomics and Epigenomics Core Facility at the Weill Cornell Medical College.

RNA-Seq read processing. Raw RNA-Seq reads were first processed to trim adapter and low-quality bases using Trimmomatic (80), and trimmed reads shorter than 40 bases were discarded. Reads mapping to rRNAs by bowtie (81) were removed. To analyze the viral transcriptome at different times postinfection, the final cleaned reads from each replicate sample were mapped to the AcMNPV genome (NCBI accession no. NC\_001623.1) using HISAT (82), allowing 2 mismatches. Following alignments, the number of mapped reads from each of the 156 viral genes was derived and then normalized to reads per kilobase of transcript per million mapped viral reads (RPKM), as described previously (28, 83). In addition, to examine expression of viral genes over the course of infection relative to total cellular expression, we also calculated RPKM values by dividing the number of mapped reads by the total number of mapped reads (cellular plus viral) instead of the total number of mapped viral reads only.

Expression profiling, cluster analysis, and correlation analysis. We identified the most highly expressed AcMNPV genes in T. ni midgut at various times following viral infection and compared expression patterns of grouped viral genes based on calculated RPKM values (as described above). The expression patterns of each functional grouping were compared in the midgut and Thms42 cell line using cell line data generated in a prior study (28). We performed cluster analysis on normalized read counts to examine specific patterns of viral genes expression. Hierarchical clustering was performed with Euclidean distance metric on the log<sub>2</sub>-transformed RPKM values using R software (84). Because absolute expression levels vary dramatically between the midgut and the cell line and we wanted to compare the expression levels in the overall context of the viral program of gene expression, we developed a ranked expression profiling method. Our goal was to compare expression of each individual viral gene in the context of all other viral genes. For each time point, we used RPKM values to rank each viral gene among all other viral genes. The rank position of each viral gene determined from the midgut infection was then compared with the rank position for the same gene determined from the cell line infection at each time point. Furthermore, to examine a best fit in viral infection timelines between the midgut and the cell line infections, we also performed a correlation analysis, comparing each gene's expression pattern in the midgut versus its expression pattern in the cell line and shifting timelines against each other (midgut and cell line). As the calculated midgut expression levels of viral genes at early times (6 and 12 h p.i.) had high standard deviations, we limited this analysis to 18 to 48 h p.i. For the cell line expression patterns, three different ranges were used: 6 to 24 h p.i., 12 to 36 h p.i., and 18 to 48 h p.i. Correlations of the expression patterns of genes between the midgut and the cell line at each set of timeline comparisons were analyzed by employing Pearson's correlation coefficient (R). For each timeline comparison (midgut at 18 to 48 h p.i. versus cell line at 6 to 24 h p.i., midgut at 18 to 48 h p.i. versus cell line at 12 to 36 h p.i., and midgut at 18 to 48 h p.i. versus cell line at 18 to 48 h p.i.), the calculated R value ranged between -1 to +1, where -1 represented a negative correlation and +1 represented a positive correlation.

**Accession number(s).** The raw RNA-Seq data were deposited in the NCBI Sequence Read Archive under accession number SRP156551.

## SUPPLEMENTAL MATERIAL

Supplemental material for this article may be found at https://doi.org/10.1128/JVI .01277-18.

**SUPPLEMENTAL FILE 1, PDF file, 0.3 MB. SUPPLEMENTAL FILE 2, XLSX file, 0.2 MB.** 

## **ACKNOWLEDGMENTS**

We thank Jenny Z. Xiang for help and assistance with Illumina sequencing, Wendy Kain for assistance with *T. ni* eggs and larvae, and Yimin Xu for generous help and support with RNA-Seq library preparation.

This work was supported by grants from the USDA (2015-67013-23281) to G.W.B., P.W., and Z.F. and from the NSF (IOS-1354421 and 1653021) to G.W.B.

## REFERENCES

- van Oers MM, Vlak JM. 2007. Baculovirus genomics. Curr Drug Targets 8:1051–1068. https://doi.org/10.2174/138945007782151333.
- ICTV. 2016. Virus taxonomy: 2016 release. https://talk.ictvonline.org/ taxonomy/.
- Ayres MD, Howard SC, Kuzio J, Lopez-Ferber M, Possee RD. 1994. The complete DNA sequence of *Autographa californica* nuclear polyhedrosis virus. Virology 202:586 – 605. https://doi.org/10.1006/viro.1994 .1380.

- O'Reilly DR, Miller LK, Luckow VA. 1992. Baculovirus expression vectors, a laboratory manual. WH Freeman and Co, New York, NY.
- Cox MM. 2012. Recombinant protein vaccines produced in insect cells. Vaccine 30:1759–1766. https://doi.org/10.1016/j.vaccine.2012.01.016.
- Felberbaum RS. 2015. The baculovirus expression vector system: a commercial manufacturing platform for viral vaccines and gene therapy vectors. Biotechnol J 10:702–714. https://doi.org/10.1002/biot .201400438.
- Martignoni ME, Iwai PJ. 1986. A catalog of viral diseases of insects, mites, and ticks, 4th ed. General technical report PNW-195. USDA Forest Service, Pacific Northwest Research Station, Portland, OR.
- Herniou EA, Jehle JA. 2007. Baculovirus phylogeny and evolution. Curr Drug Targets 8:1043–1050. https://doi.org/10.2174/138945007782151306.
- Nealis VG, Turnquist R, Morin B, Graham RI, Lucarotti CJ. 2015. Baculoviruses in populations of western spruce budworm. J Invertebr Pathol 127:76–80. https://doi.org/10.1016/j.jip.2015.03.005.
- Moreau G, Lucarotti CJ. 2007. A brief review of the past use of baculoviruses for the management of eruptive forest defoliators and recent developments on a sawfly virus in Canada. Forestry Chronicle 83: 105–112. https://doi.org/10.5558/tfc83105-1.
- Popham HJ, Nusawardani T, Bonning BC. 2016. Introduction to the use of baculoviruses as biological insecticides. Methods Mol Biol 1350: 383–392. https://doi.org/10.1007/978-1-4939-3043-2\_19.
- Blissard GW, Theilmann DA. 2018. Baculovirus entry and egress from insect cells. Annu Rev Virol 5:113–139. https://doi.org/10.1146/annurev -virology-092917-043356.
- Wang P, Granados RR. 1997. An intestinal mucin is the target substrate for a baculovirus enhancin. Proc Natl Acad Sci U S A 94:6977–6982.
- Horton HM, Burand JP. 1993. Saturable attachment sites for polyhedronderived baculovirus on insect cells and evidence for entry via direct membrane fusion. J Virol 67:1860 – 1868.
- Peng K, van Oers MM, Hu Z, van Lent JWM, Vlak JM. 2010. Baculovirus per os infectivity factors form a complex on the surface of occlusion-derived virus. J Virol 84:9497–9504. https://doi.org/10.1128/JVI.00812-10.
- Peng K, van Lent JW, Boeren S, Fang M, Theilmann DA, Erlandson MA, Vlak JM, van Oers MM. 2012. Characterization of novel components of the baculovirus per os infectivity factor complex. J Virol 86:4981–4988. https://doi.org/10.1128/JVI.06801-11.
- Wang X, Liu X, Makalliwa GA, Li J, Wang H, Hu Z, Wang M. 2017. Per os infectivity factors: a complicated and evolutionarily conserved entry machinery of baculovirus. Sci China Life Sci 60:806–815. https://doi.org/ 10.1007/s11427-017-9127-1.
- Boogaard B, van Oers MM, van Lent JWM. 2018. An advanced view on baculovirus per os infectivity factors. Insects 9:E84. https://doi.org/10 .3390/insects9030084.
- Au S, Wu W, Zhou L, Theilmann DA, Pante N. 2016. A new mechanism for nuclear import by actin-based propulsion used by a baculovirus nucleocapsid. J Cell Sci 129:2905–2911. https://doi.org/10.1242/jcs.191668.
- Au S, Wu W, Pante N. 2013. Baculovirus nuclear import: open, nuclear pore complex (NPC) sesame. Viruses 5:1885–1900. https://doi.org/10 .3390/v5071885.
- Rohrmann GF. 2013. Baculovirus molecular biology, 3rd ed. National Center for Biotechnology Information, Bethesda, MD. http://www.ncbi .nlm.nih.gov/pubmed/24479205.
- Engelhard EK, Kam-Morgan LNW, Washburn JO, Volkman LE. 1994. The insect tracheal system: a conduit for the systemic spread of *Autographa* californica M nuclear polyhedrosis virus. Proc Natl Acad Sci U S A 91:3224–3227.
- Flipsen JT, Martens JW, van Oers MM, Vlak JM, van Lent JW. 1995. Passage of Autographa californica nuclear polyhedrosis virus through the midgut epithelium of Spodoptera exigua larvae. Virology 208: 328–335. https://doi.org/10.1006/viro.1995.1156.
- Granados RR, Lawler KA. 1981. In vivo pathway of Autographa californica baculovirus invasion and infection. Virology 108:297–308. https://doi.org/10.1016/0042-6822(81)90438-4.
- Washburn JO, Chan EY, Volkman LE, Aumiller JJ, Jarvis DL. 2003. Early synthesis of budded virus envelope fusion protein GP64 enhances Autographa californica multicapsid nucleopolyhedrovirus virulence in orally infected Heliothis virescens. J Virol 77:280–290. https://doi.org/10 .1128/JVI.77.1.280-290.2003.
- Passarelli AL. 2011. Barriers to success: how baculoviruses establish efficient systemic infections. Virology 411:383–392. https://doi.org/10 .1016/j.virol.2011.01.009.
- 27. Means JC, Passarelli AL. 2010. Viral fibroblast growth factor, matrix

- metalloproteases, and caspases are associated with enhancing systemic infection by baculoviruses. Proc Natl Acad Sci U S A 107:9825–9830. https://doi.org/10.1073/pnas.0913582107.
- Chen YR, Zhong S, Fei Z, Hashimoto Y, Xiang JZ, Zhang S, Blissard GW. 2013. The transcriptome of the baculovirus *Autographa californica* multiple nucleopolyhedrovirus (AcMNPV) in *Trichoplusia ni* cells. J Virol 87:6391–6405. https://doi.org/10.1128/JVI.00194-13.
- Garrity DB, Chang M-J, Blissard GW. 1997. Late promoter selection in the baculovirus gp64 envelope fusion protein gene. Virology 231:167–181. https://doi.org/10.1006/viro.1997.8540.
- Blissard GW, Rohrmann GF. 1990. Baculovirus diversity and molecular biology. Annu Rev Entomol 35:127–155. https://doi.org/10.1146/annurev.en.35.010190.001015.
- Thiem SM, Miller LK. 1989. Identification, sequence, and transcriptional mapping of the major capsid protein gene of the baculovirus *Autogra*pha californica nuclear polyhedrosis virus. J Virol 63:2008 –2018.
- Rankin C, Ooi BG, Miller LK. 1988. Eight base pairs encompassing the transcriptional start point are the major determinant for baculovirus polyhedrin gene expression. Gene 70:39–49. https://doi.org/10.1016/ 0378-1119(88)90102-3.
- Clem RJ. 2007. Baculoviruses and apoptosis: a diversity of genes and responses. Curr Drug Targets 8:1069–1074. https://doi.org/10.2174/ 138945007782151405.
- O'Reilly DR, Miller LK. 1989. A baculovirus blocks insect molting by producing ecdysteroid UDP-glucosyl transferase. Science 245: 1110–1112. https://doi.org/10.1126/science.2505387.
- Clem RJ, Fechheimer M, Miller LK. 1991. Prevention of apoptosis by a baculovirus gene during infection of insect cells. Science 254: 1388–1390. https://doi.org/10.1126/science.1962198.
- Hoover K, Grove M, Gardner M, Hughes DP, McNeil J, Slavicek J. 2011. A gene for an extended phenotype. Science 333:1401. https://doi.org/10 .1126/science.1209199.
- van Houte S, Ros VI, van Oers MM. 2014. Hyperactivity and tree-top disease induced by the baculovirus AcMNPV in Spodoptera exigua larvae are governed by independent mechanisms. Naturwissenschaften 101:347–350. https://doi.org/10.1007/s00114-014-1160-8.
- Kamita SG, Nagasaka K, Chua JW, Shimada T, Mita K, Kobayashi M, Maeda S, Hammock BD. 2005. A baculovirus-encoded protein tyrosine phosphatase gene induces enhanced locomotory activity in a lepidopteran host. Proc Natl Acad Sci U S A 102:2584–2589. https://doi.org/ 10.1073/pnas.0409457102.
- Ooi BG, Miller LK. 1988. Regulation of host RNA levels during baculovirus infection. Virology 166:515–523. https://doi.org/10.1016/0042-6822(88)905 22-3.
- Chen YR, Zhong S, Fei Z, Gao S, Zhang S, Li Z, Wang P, Blissard GW. 2014. Transcriptome responses of the host Trichoplusia ni to infection by the baculovirus Autographa californica multiple nucleopolyhedrovirus. J Virol 88:13781–13797. https://doi.org/10.1128/JVI.02243-14.
- Hou D, Zhang L, Deng F, Fang W, Wang R, Liu X, Guo L, Rayner S, Chen X, Wang H, Hu Z. 2013. Comparative proteomics reveal fundamental structural and functional differences between the two progeny phenotypes of a baculovirus. J Virol 87:829–839. https://doi.org/10.1128/JVI .02329-12.
- Braunagel SC, Russell WK, Rosas-Acosta G, Russell DH, Summers MD. 2003. Determination of the protein composition of the occlusionderived virus of *Autographa californica* nucleopolyhedrovirus. Proc Natl Acad Sci U S A 100:9797–9802.
- Evans JT, Rohrmann GF. 1997. The baculovirus single-stranded DNA binding protein, LEF-3, forms a homotrimer in solution. J Virol 71: 3574–3579.
- Wu Y, Carstens EB. 1998. A baculovirus single-stranded DNA binding protein, LEF-3, mediates the nuclear localization of the putative helicase P143. Virology 247:32–40. https://doi.org/10.1006/viro.1998.9235.
- Mikhailov VS, Okano K, Rohrmann GF. 2003. Baculovirus alkaline nuclease possesses a 5'→3' exonuclease activity and associates with the DNA-binding protein LEF-3. J Virol 77:2436–2444. https://doi.org/10.1128/JVI.77.4.2436-2444.2003.
- Beames B, Summers MD. 1989. Location and nucleotide sequence of the 25k protein missing from baculovirus few polyhedra FP mutants. Virology 168:344–353. https://doi.org/10.1016/0042-6822(89)90275-4.
- Harrison RL, Jarvis DL, Summers MD. 1996. The role of the AcMNPV 25K gene, "FP25," in baculovirus polh and p10 expression. Virology 226: 34–46. https://doi.org/10.1006/viro.1996.0625.
- 48. Fraser MJ, Brusca JS, Smith GE, Summers MD. 1985. Transposon medi-

- ated mutagenesis of a baculovirus. Virology 145:356–361. https://doi.org/10.1016/0042-6822(85)90172-2.
- Kool M, Ahrens CH, Goldbach RW, Rohrmann GF, Vlak JM. 1994. Identification of genes involved in DNA replication of the *Autographa californica* baculovirus. Proc Natl Acad Sci U S A 91:11212–11216. https://doi.org/10.1073/pnas.91.23.11212.
- Hang X, Dong W, Guarino LA. 1995. The *lef-3* gene of *Autographa calfonica* nuclear polyhedrosis virus encodes a single-stranded DNA-binding protein. J Virol 69:3924–3928.
- Yu M, Carstens EB. 2010. Identification of a domain of the baculovirus AcMNPV single-strand DNA binding protein LEF-3 essential for viral DNA replication. J Virol 84:6153–6162. https://doi.org/10.1128/JVI.00115-10.
- Okano K, Vanarsdall AL, Rohrmann GF. 2007. A baculovirus alkaline nuclease knockout construct produces fragmented DNA and aberrant capsids. Virology 359:46–54. https://doi.org/10.1016/j.virol.2006.09.008.
- Mikhailov VS, Okano K, Rohrmann GF. 2004. Specificity of the endonuclease activity of the baculovirus alkaline nuclease for singlestranded DNA. J Biol Chem 279:14734–14745. https://doi.org/10 .1074/jbc.M311658200.
- Li L, Rohrmann GF. 2000. Characterization of a baculovirus alkaline nuclease. J Virol 74:6401–6407. https://doi.org/10.1128/JVI.74.14.6401 -6407.2000
- Javed MA, Harris S, Willis LG, Theilmann DA, Donly BC, Erlandson MA, Hegedus DD. 2016. Microscopic investigation of AcMNPV infection in the *Trichoplusia ni* midgut. J Invertebr Pathol 141:24–33. https://doi.org/10 .1016/j.jip.2016.10.006.
- Volkman LE, Summers MD. 1977. Autographa californica nuclear polyhedrosis virus: comparative infectivity of the occluded, alkali-liberated, and nonoccluded forms. J Invertebr Pathol 30:102–103. https://doi.org/10.1016/0022-2011(77)90045-3.
- 57. Bonfini A, Liu X, Buchon N. 2016. From pathogens to microbiota: how Drosophila intestinal stem cells react to gut microbes. Dev Comp Immunol 64:22–38. https://doi.org/10.1016/j.dci.2016.02.008.
- Sansone CL, Cohen J, Yasunaga A, Xu J, Osborn G, Subramanian H, Gold B, Buchon N, Cherry S. 2015. Microbiota-dependent priming of antiviral intestinal immunity in Drosophila. Cell Host Microbe 18:571–581. https:// doi.org/10.1016/j.chom.2015.10.010.
- Kang WK, Imai N, Suzuki M, Iwanaga M, Matsumoto S, Zemskov EA. 2003. Interaction of Bombyx mori nucleopolyhedrovirus BRO-A and host cell protein laminin. Arch Virol 148:99 –113. https://doi.org/10.1007/s00705 -002-0902-7.
- Roncarati R, Knebel-Moersdorf D. 1997. Identification of the early actinrearrangement-inducing factor gene, arif-1, from Autographa californica multicapsid nuclear polyhedrosis virus. J Virol 71:7933–7941. (Erratum, 72:888–889, 1998.)
- Dreschers S, Roncarati R, Knebel-Moersdorf D. 2001. Actin rearrangement-inducing factor of baculoviruses is tyrosine phosphorylated and colocalizes to F-actin at the plasma membrane. J Virol 75: 3771–3778. https://doi.org/10.1128/JVI.75.8.3771-3778.2001.
- Charlton CA, Volkman LE. 1991. Sequential rearrangement and nuclear polymerization of actin in baculovirus-infected Spodoptera frugiperda cells. J Virol 65:1219–1227.
- Kokusho R, Kawamoto M, Koyano Y, Sugano S, Suzuki Y, Shimada T, Katsuma S. 2015. Bombyx mori nucleopolyhedrovirus actin rearrangement-inducing factor 1 enhances systemic infection in B. mori larvae. J Gen Virol 96:1938–1946. https://doi.org/10.1099/vir.0.000130.
- Zhang Y, Hu X, Mu J, Hu Y, Zhou Y, Zhao H, Wu C, Pei R, Chen J, Chen X, Wang Y. 2018. Ac102 participates in nuclear actin polymerization by modulating BV/ODV-C42 ubiquitination during Autographa californica multiple nucleopolyhedrovirus infection. J Virol 92:e00005–18. https://doi.org/10.1128/JVI.00005-18.
- Gandhi KM, Ohkawa T, Welch MD, Volkman LE. 2012. Nuclear localization of actin requires AC102 in Autographa californica multiple nucleopolyhedrovirus-infected cells. J Gen Virol 93:1795–1803. https://doi.org/10.1099/vir.0.041848-0.

 Ohkawa T, Rowe AR, Volkman LE. 2002. Identification of six Autographa californica multicapsid nucleopolyhedrovirus early genes that mediate nuclear localization of G-actin. J Virol 76:12281–12289. https://doi.org/ 10.1128/JVI.76.23.12281-12289.2002.

- Hepp SE, Borgo GM, Ticau S, Ohkawa T, Welch MD. 2018. Baculovirus AC102 is a nucleocapsid protein that is crucial for nuclear actin polymerization and nucleocapsid morphogenesis. J Virol 92:e00111–18. https://doi.org/10.1128/JVI.00111-18.
- Lehiy CJ, Martinez O, Passarelli AL. 2009. Virion-associated viral fibroblast growth factor stimulates cell motility. Virology 395:152–160. https://doi.org/10.1016/j.virol.2009.09.011.
- Detvisitsakun C, Cain EL, Passarelli AL. 2007. The Autographa californica M nucleopolyhedrovirus fibroblast growth factor accelerates host mortality. Virology 365:70–78. https://doi.org/10.1016/j.virol.2007.03.027.
- Katsuma S, Horie S, Daimon T, Iwanaga M, Shimada T. 2006. In vivo and in vitro analyses of a Bombyx mori nucleopolyhedrovirus mutant lacking functional vfgf. Virology 355:62–70. https://doi.org/10.1016/j.virol.2006 .07.008.
- Katsuma S, Daimon T, Mita K, Shimada T. 2006. Lepidopteran ortholog of Drosophila breathless is a receptor for the baculovirus fibroblast growth factor. J Virol 80:5474–5481. https://doi.org/10.1128/JVI.00248-06.
- Detvisitsakun C, Hutfless EL, Berretta MF, Passarelli AL. 2006. Analysis of a baculovirus lacking a functional viral fibroblast growth factor homolog. Virology 346:258–265. https://doi.org/10.1016/j.virol.2006.01.016.
- Detvisitsakun C, Berretta MF, Lehiy C, Passarelli AL. 2005. Stimulation of cell motility by a viral fibroblast growth factor homolog: proposal for a role in viral pathogenesis. Virology 336:308–317. https://doi.org/10 .1016/j.virol.2005.03.013.
- Yin F, Du R, Kuang W, Yang G, Wang H, Deng F, Hu Z, Wang M. 2016. Characterization of the viral fibroblast growth factor homolog of Helicoverpa armigera single nucleopolyhedrovirus. Virol Sin 31:240–248. https://doi.org/10.1007/s12250-016-3710-z.
- Yu IL, Bray D, Lin YC, Lung O. 2009. Autographa californica multiple nucleopolyhedrovirus ORF 23 null mutant produces occlusion-derived virions with fewer nucleocapsids. J Gen Virol 90:1499–1504. https://doi.org/10.1099/vir.0.009035-0.
- Granados RR, Li GX, Derksen ACG, Mckenna KA. 1994. A new insect cell line from *Trichoplusia ni* (BTI-Tn-5B1-4) susceptible to *Trichoplusia ni* single enveloped nuclear polyhedrosis virus. J Invertebr Pathol 64: 260–266. https://doi.org/10.1016/S0022-2011(94)90400-6.
- 77. Hink WF. 1970. Established insect cell line from the cabbage looper, *Trichoplusia ni*. Nature 226:466–467.
- Ohkawa T, Volkman LE, Welch MD. 2010. Actin-based motility drives baculovirus transit to the nucleus and cell surface. J Cell Biol 190: 187–195. https://doi.org/10.1083/icb.201001162.
- Zhong S, Joung JG, Zheng Y, Chen YR, Liu B, Shao Y, Xiang JZ, Fei Z, Giovannoni JJ. 2011. High-throughput Illumina strand-specific RNA sequencing library preparation. Cold Spring Harb Protoc 2011:940–949. https://doi.org/10.1101/pdb.prot5652.
- Bolger AM, Lohse M, Usadel B. 2014. Trimmomatic: a flexible trimmer for Illumina sequence data. Bioinformatics 30:2114–2120. https://doi.org/10 .1093/bioinformatics/btu170.
- Langmead B. 2010. Aligning short sequencing reads with Bowtie. Curr Protoc Bioinformatics Chapter 11:Unit 11.17.
- Kim D, Langmead B, Salzberg SL. 2015. HISAT: a fast spliced aligner with low memory requirements. Nat Methods 12:357–360. https://doi.org/10 .1038/nmeth.3317.
- Mortazavi A, Williams BA, McCue K, Schaeffer L, Wold B. 2008. Mapping and quantifying mammalian transcriptomes by RNA-Seq. Nat Methods 5:621–628. https://doi.org/10.1038/nmeth.1226.
- Love MI, Huber W, Anders S. 2014. Moderated estimation of fold change and dispersion for RNA-seq data with DESeq2. Genome Biol 15:550. https://doi.org/10.1186/s13059-014-0550-8.